SURFACE MODIFICATION: UNIQUE ELLIPSOIDAL/STROBILI-FIBER STRUCTURE OF POROUS CARBON MONOLITH FOR ELECTRODE SUPERCAPACITOR

by Rika Taslim

Submission date: 01-May-2023 08:49PM (UTC+0700)
Submission ID: 2080916472
File name: NanoScience_and_NanoTechnology_2021.pdf (6.5M)
Word count: 8504
Character count: 44965

Nanoscience and Technology: An International Journal 12(4):45–63 (2021)

SURFACE MODIFICATION: UNIQUE ELLIPSOIDAL/STROBILI-FIBER STRUCTURE OF POROUS CARBON MONOLITH FOR ELECTRODE SUPERCAPACITOR

Erman Taer,[1,]* Apriwandi,[1] Agustino,[1] Rika Taslim,[2] Widya Sinta Mustika,[1] & Exa Fadli[1]

[1]*Department of Physics, Faculty of Mathematic and Natural Sciences, University of Riau, 28293 Simpang Baru, Riau, Indonesia*

[2]*Department of Industrial Engineering, State Islamic University of Sultan Syarif Kasim, 28293 Simpang Baru, Riau, Indonesia*

*Address all correspondence to: Erman Taer, Department of Physics, Faculty of Mathematic and Natural Sciences, University of Riau, 28293 Simpang Baru, Riau, Indonesia; Tel.: +62 81275214501, E-mail: erman.taer@lecturer.unri.ac.id; erman_taer@yahoo.com

Original Manuscript Submitted: 1/21/2021; Final Draft Received: 5/7/2021

A modification of the surface morphology of activated carbon using a unique ellipsoidal/strobili-fiber structure is successfully synthesized from cocoa shell waste through one-stage pyrolysis and zinc chloride impregnation. The porous carbon maintained a monolith form without the addition of adhesive materials. According to this method, the unique combination of ellipsoidal, strobili-fiber, and rod-like structures provided the highest specific surface area and abundant micropores and mesopores. In combination with the high carbon content of 92.71% and specific surface area of 619.717 m^2/g^{-1}, the mesoporous activated carbon 0.5 (MAC-0.5) samples exhibited a high specific capacitance of 210 F/g^{-1} per 1 M of sulfuric acid electrolytes. Furthermore, the energy density of the assembled symmetrical supercapacitor was as high as 29.16 $(W{\cdot}h)/kg^{-1}$ with a power density of 105.08 W/kg^{-1} in the two-electrode system. Therefore, these results indicate that due to the electrochemical properties of activated carbon, cocoa shell waste can be highly recommended as a potential material for use energy storage applications.

KEY WORDS: *ellipsoidal/strobili-fiber structure, porous activated carbon, electrode materials, supercapacitor*

1. INTRODUCTION

The constant growth of the world's population and economic and social developments are the main factors in the increasing demand for global energy, which is currently provided from fossil fuels (Bilandzija et al., 2018; Abbas et al., 2019). It is estimated that energy consumption will increase by around 48% by the year 2040 (Avcıoğlu et al., 2019), and will continue to increase about six times during this century (Kumar and Samadder, 2017). Therefore, ensuring access to affordable, reliable, sustainable, and modern energy is a major problem for the world today. Biomass-based energy storage technology, especially in relation to agricultural and agro-industrial waste, is the best solution to reducing

2572-4258/21/$35.00

the cost of renewable energy (Liu et al., 2017; Rountree, 2019). Numerous research studies have reported article reviews as well as studies on the high potential of biomass waste as a raw material for energy storage (Dessie et al., 2019), especially for supercapacitors (Liu et al., 2018; Wang et al., 2019). The supercapacitor is an electrochemical energy storage technology that can produce high power and energy compared to other devices such as batteries and conventional capacitors (Simon and Burke, 2008; González et al., 2016). Basically, supercapacitors perform better than conventional or battery capacitors. Supercapacitors can store more energy than capacitors and have more power than batteries. However, supercapacitors still have shortcomings, such as high production costs and the fact that the high-power energy produced is still not balanced (González-García, 2018; Miller et al., 2018). To answer this challenge, researchers have developed and modified electrode materials, which is a main factor in the performance of a supercapacitor (Poonam et al., 2019). Increasing the specific energy in a supercapacitor requires an electrode material that has a combination of pores, including micropores, mesopores, and macropores (Zhang et al., 2017; Fu et al., 2018). These pores have their respective contributions to improving the performance of supercapacitors. Macropores provide a relatively short distance for ion diffusion on the surface of the electrode material (Zhang et al., 2017). Mesopores provide a relatively unhindered ion transport pathway to the electrode/electrolyte interface (Jain et al., 2015). Furthermore, micropores provide a high surface area, allowing more electric double layers to form (Gou et al., 2020). The combination of these three pores can achieve higher supercapacitor performance.

A few researchers have recommended using the unique structure of nanomaterials to achieve a good combination of pores, such as rod-like, strobili-fiber, and ellipsoidal structures (Dehkhoda et al., 2016; Jiang et al., 2019; Taer et al., 2021). Sun et al. (2018) performed experiments on the unique ellipsoidal porous structure for a supercapacitor, which enhanced the specific capacitance as high as 306.4 F/g^{-1}. Furthermore, hierarchical porous rod-like carbon, which is derived from aluminum-based metal organic frameworks, has shown higher electrochemical behavior of 345 F/g^{-1}, as reported in Jiang et al. (2019). However, these unique structures are obtained by complex methods, multi-step processes, and the addition of synthetic materials, metal frameworks, and templates. Recently, the results of a study on the unique structure of a rod-like nanomaterial of activated carbon derived from agricultural and agro-industrial waste by relatively simple methods without any templates or metal framework were reported (Taer et al., 2021), in which the experiemnest were performed at a relatively high specific energy of 26.90 $(W{\cdot}h)/kg^{-1}$. However, not all biomass waste can be potentially used to provide a unique nanostructure in carbon electrode materials. Therefore, it is necessary to know the biomass criteria that allow producing nanostructures through a simple method and do not require the addition of other synthetic materials.

Worldwide, agricultural and agro-industrial waste is increasing every year by 5%–10% (Wang et al., 2016). One of the crops that contributes to high biomass waste is the cocoa co-product. Cacao (*Theobroma cacao L.*) is a small cocoa tree in the Malvaceae family. Cocoa beans are used to make liquor, cocoa solids, butter, and chocolate (Okiyama et al., 2017). The world production of cocoa beans in the 2018/2019 harvest

was 422,900 thousand tons, and it is estimated that there will be an increase of 2.1% in 2019/2020 (cocoa prepared on June 2, 2020, by Foresight Commodity Services, Inc., Lisle, IL). The countries that produce cocoa beans are the Ivory Coast, Ghana, Ecuador, Cameroon, Nigeria, Indonesia, and Brazil, contributing to almost 90% of the world production (cocoa prepared on June 2, 2020, by Foresight Commodity Services, Inc., Lisle, IL). The high production rates will certainly increase waste products, such as husks and shells. The presence of shells in products made from cocoa beans is undesirable because it adversely affects the process and quality (Vásquez et al., 2019). However, the cocoa shell contains rich-lignocellulose consisting of hemicellulose, cellulose, and lignin at 35.26%, 41.92%, and 0.95%, respectively, which indicates the shell has great potential as an activated carbon base material with a high surface area, suitable pore size, and unique morphological structure for enhanced supercapacitor performance (Gao et al., 2017; Thomas et al., 2019). Many researchers have reported results on the conversion of cocoa shells to activated carbon by various methods (Ahmad et al., 2013; Fioresi et al., 2017; Pereira et al., 2014).

In general, biomass waste can be converted to activated carbon for supercapacitors through carbonization and activation. There are three commonly used activation methods: (1) physical activation using gases, (2) chemical activation through the addition of different compounds, and (3) a combination of both physical and chemical activation (González et al., 2016; Miller et al., 2018; Jose et al., 2019). Ahmad et al. (2013) reported that activated carbon from the cocoa shells through physical activation can be done by flowing carbon dioxide (CO_2) gas up to 800°C (Ahmad et al., 2013). The specific surface area produced is 558.3 m^2/g^{-1}. Similarly, it was reported by other researchers that activated carbon can be obtained from cacao shells by using different chemicals such as phosphoric acid (H_3PO_4) and zinc chloride ($ZnCl_2$) (Pereira et al., 2014; Jawad et al., 2020; Kirbiyik et al., 2017). The resulting surface areas are higher by 642 and 1077 m^2/g^{-1}, respectively, with an average pore diameter in the range of 2.3–2.6 nm. Furthermore, Yetri et al. (2020) successfully converted cocoa shell activated carbon into a supercapacitor electrode through multi-activation of both physical and chemical methods at a specific capacitance of 90.2 F/g^{-1} (Yetri et al., 2020). However, the pore structure, structural morphology, and specific capacitance generated in previous studies have not greatly improved supercapacitor performance.

In this study, a cost-efficient and eco-friendly strategy was adopted to produce a unique structure of porous activated carbon, which exhibited a monolith-type form, by using agricultural and agro-industrial waste from cocoa shells as the raw material through single-step pyrolysis and $ZnCl_2$ activation. Low concentrations of $ZnCl_2$ were added during the process to retain the self-adhesive behavior of the precursor, which facilitated the conversion of the carbon powder into the monolith form without an adhesive material. As a result, the activated carbon obtained a unique structure of ellipsoidal, strobili-fiber, and rod-like shapes, which ensured improved specific capacitance and suitable pore size. Furthermore, the electrochemical properties exhibited a specific capacitance as high as 210 F/g^{-1} at a low scanning rate in the 1 M sulfuric acid (H_2SO_4) electrolyte at high specific energy of 29.16 $(W \cdot h)/kg^{-1}$. This confirmed the high potential

of cocoa shell waste in forming the unique structure of ellipsoidal, strobili-fiber activated carbon, which can be used in electrochemical energy storage applications.

2. EXPERIMENTAL SECTION

2.1 Materials

The cacao shell waste (in the form of 5 ×5 cm small pieces) was acquired from a Pekanbaru traditional market. The shell waste was dried for a few days and pre-carbonized at 250°C in a vacuum oven for 2.5 hours. Subsequently, the shell waste was converted into powder by a mortar decanter and a milling tool and then sieved to obtain a powder with a particle size of < 53 µm. Zinc chloride and sulfuric acid were obtained from Merck KGaA (Darmstadt, Germany).

2.2 Preparation of the Activated Carbon

The mesoporous activated carbon (MAC) samples were prepared by one-stage integrated pyrolysis. The pre-carbonized cacao shell powder (30 g) was impregnated with $ZnCl_2$ solution (0.05 m/L^{-1}) by using a hot plate and magnetic stirrer at 300 rotations per minute for 2 hours and then dried in a vacuum oven for 2 days. Subsequently, the dried, impregnated powder samples were converted into monoliths with diameters of ± 2 cm by pressing 8 tons of hydraulic press instruments. Then, this obtained output was pyrolyzed by using both carbonization and physical activation in a furnace tube. The carbonization process was performed in nitrogen (N_2) gas at temperatures from 30°C to 600°C, accompanied by physical activation in CO_2 atmosphere, which was simultaneously set at 850°C for 2 hours. The flow rate of the N_2/CO_2 gas and the increases in the carbonization and physical temperatures represent the pyrolysis profile shown in Fig. 1. The obtained MAC products were labeled MAC-0.5. To investigate the effect of the concentration of $ZnCl_2$ on the physical and electrochemical properties of the porous activated carbon cocoa shell, experiments at concentrations of 0.1 and 0.2 m/L^{-1} were

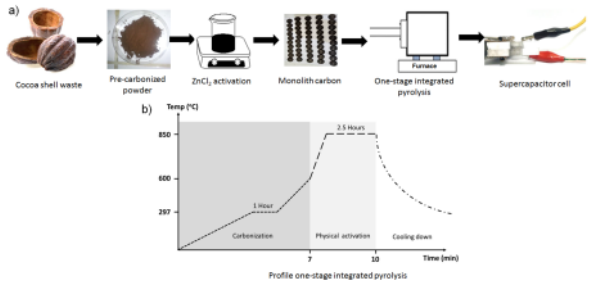

FIG. 1: Schematic illustration of the preparation of activated carbon (a) and the pyrolysis profile (b)

performed using a procedure similar to that previously described. The obtained products were labeled MAC-1 and MAC-2. Finally, the samples were neutralized by distilled water and further polished to achieve a thick electrode.

2.3 Material Characterizations

The physical properties of the activated carbon electrodes were characterized and analyzed as well as the capacitive performance. Thermogravimetric (TG) and differential thermogravimetric (DTG) analyses were performed using the Shimadzu TGA-50 TG analyzer to identify and evaluate the thermal behavior of the carbon powder. In addition, powder X-ray diffraction (XRD) was employed to characterize the microstructure of the samples by using the Phillip X-Pert Pro PW3060/10 instrument with Cu Kα radiation (α = 1.5418 Å) in the scanning range of 10°–100°. The average interlayer spacings (d_{002} and d_{100}) were obtained using Bragg's law, while the microcrystalline dimensions (L_c and L_a) were calculated using the Debey–Scherer equation. Furthermore, scanning electron microscope (SEM) micrograph and energy-dispersive spectroscopy (EDS) images were collected with the JEOL JSM-6510 LA instrument at a working voltage of 15 kV to observe the morphological structure and elemental elements of the samples. The porosity behaviors, including the specific surface area and pore size distributions, were exhibited through N_2 adsorption–desorption measurements obtained with the Quantachrome TouchWiz (version 1.2) instrument at a liquid temperature of 77 K.

2.4 Electrochemical Measurement

The electrochemical performance of the strobili-fiber activated carbon, which were prepared through single-step pyrolysis and chemical activation, was investigated using a two-electrode system with a duck egg shell as the separator. The capacitive performance was investigated using the cyclic voltammetry (CV) technique and the CV-UR Rad-Er 5841 instrument. This instrument was calibrated by VersaStat II Princeton Applied Research with an average error value ± 6.0%. The CV technique was performed at a low scanning rate in the range of 1–10 mV/s^{-1} with a potential window of 0.0–1.0 V, in which 1 M H_2SO_4 was selected as the aqueous electrolyte. Furthermore, the specific capacitance, specific energy, and specific power were calculated by standard equations as follows (Sun et al., 2019; Men et al., 2019):

$$C_{sp} = \frac{2 \cdot I}{s \cdot m} \tag{1}$$

$$E = \frac{1}{2} \cdot C_{sp} \cdot V^2 \cdot \frac{1000}{3600} \tag{2}$$

$$P = \frac{E}{\Delta t} \cdot 3600 \tag{3}$$

where I is the average current density; m is the electrode mass loading; s is the scanning rate; V is the voltage window; Δt is the charge/discharge time process; C_{sp} is the specific capacitance; E is the specific energy; and P is the specific power.

3. RESULTS AND DISCUSSION

3.1 Thermal Properties

Single-step pyrolysis, including N_2 carbonization and CO_2 activation, is an important factor in the process of changing cocoa shells into activated carbon powder. The pyrolysis process aim to evaporate the moisture and volatile to exhibited high carbon fixed and developed the suitable pore size for electrode materials (González-García, 2018). The TG-DTG curve, as shown in Fig. 2, can be used to create a pyrolysis profile. According to the TG curve, significant weight loss can be classified as occurring in three stages. The first stage occurs before the temperature reaches 200°C with weight loss of 6.75%, which is related to the moisture evaporation and water decomposition in the cocoa shell (Saka, 2012; Qu et al., 2015). The second stage occurs at 200–400°C with mass loss of 32.24%, which is mostly consistent with the decomposition of the gaseous products in complex compounds (e.g., hemicellulose, cellulose, and lignin) and small CO_2 molecules in the thermal rearrangement reaction (Fan et al., 2017; González et al., 2009). In this stage, lignocellulose disintegrates and breaks down to form a regular structure. The third stage occurs in the temperature range of 500–600°C with weight-loss as high as 49.73% of the original mass observed in the TG curve, and describes the main chain of the macromolecules and heteroatoms of the raw materials (Lin et al., 201[42] The pyrolysis profile is presented in detail in Fig. 1(b), where the TG curve shows the weig[42] loss rate of the cocoa shell. Figure 1(b) indicates there was no dramatic change in the weight-loss rate in the temperature range of 30–250°C; however, when the pyrolysis temperature reached 297.5°C the weight-loss rate increase by 0.179 mg/min, which is consistent with the second stage of the TG curve. This phenomenon was indicated by the degradation of lignocellulosic compounds, which occurred simultaneously by deep thermolysis of polysaccharides (Lin et al., 2019; González et al., 2009; Uysal et al., 2014), although no temperature decrease was observed due to mass loss. Therefore, 297.6°C was used as an initial method of carbonizing the holding temperature. The selection of

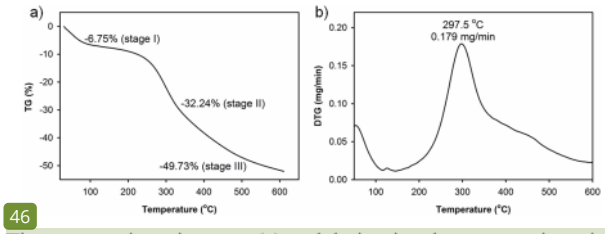

[46] **FIG. 2:** Thermo-gravimetric curve (a) and derivative thermo-gravimetric curve (b)

initial and maximum carbonization temperatures should decompose the lignocellulose compounds and modify the structure of porous carbon, which is advantageous for the performance of supercapacitor electrodes.

3.2 Degree of Crystallinity Analysis

The degree of crystallinity of the MAC samples was observed by XRD characterization. Figure 3 presents the MAC-0.5, MAC-1, and MAC-2 XRD curves, which shows that there are broadening diffraction peaks centered at 2θ angles of approximately 24–25° and 44–46° for the (002) and (100) lattice planes of graphite crystal, respectively (Boyjoo et al., 2017). The two large peaks demonstrate the amorphous properties of small crystals. The strong diffraction peaks (002) imply that the MAC samples had a graphite-like structure. The slight diffraction peak (100) indicates that a small amount of graphite microcrystalline structure is present in the samples (Miller et al., 2018; Boyjoo et al., 2017). This was also discovered in other reports that used various precursors such as mangosteen (Li et al., 2018; Yang et al., 2019), pitaya peels (Lu et al., 2020), sakura flowers (Ma et al., 2019a), rice husks (Mai et al., 2019; Lebedeva et al., 2015), and durian shells (Taer et al., 2019), which showed broadening peaks centered at 2θ angles of approximately 24° and 44°. In addition, the diffraction plane (002) of the MAC-0.5 samples changed from 25° to 24° and the diffraction plane (100) at a larger angle changed from 44° to 47° for the MAC-1 and MAC-2 samples, respectively. This confirms that the MAC-0.5 samples had greater average interlayer spacing compared to the MAC-1 and MAC-2 samples. This case may be due to the existence of the combination of pore sizes, which included micro-, meso-, and macropores and improved the specific surface area and shortened the pathway of ion electrolytes into the electrode surface. This mainly helped to improve the performance of the supercapacitors in the MAC-0.5 samples (see

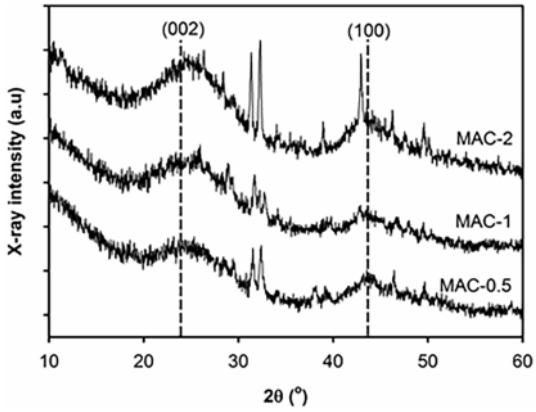

FIG. 3: XRD pattern of cocoa shell activated carbon

the N_2 adsorption and electrochemical analyses). Based on these properties, the single-step pyrolysis and 0.05 m/L^{-1} $ZnCl_2$ activation succeeded in converting the cocoa shell into monolithic porous carbon for the supercapacitor electrode. The XRD curves also showed several net peaks observed at 2θ angles of 32°, 33°, and 42° due to the presence of the crystal-like structure, which developed as a result of the potassium content from different compounds of calcium oxide (CaO) and calcium carbonate ($CaCO_3$) (JCPDS No. 82-1690). These results were also observed in the EDS analysis.

3.3 Morphological Structure Analysis

As has been widely reported, biomass waste can be converted into activated carbon using the pyrolysis of both physical and chemical activation. These processes convert the raw materials into a higher fixed carbon content by creating a certain ordering of the structure, which results in a highly porous solid of the activated carbon. This process successfully converts the cocoa shell into the porous structure of activated carbon. Figure 4 shows a randomly aggregated structure with a size range from 0.56 to 1.79 μm. Activation of $ZnCl_2$ exhibited obvious differences in the morphologies of the MAC-0.5 and MAC-2 samples, as shown in Fig. 4(a) and 4(b), respectively. Its activation in the

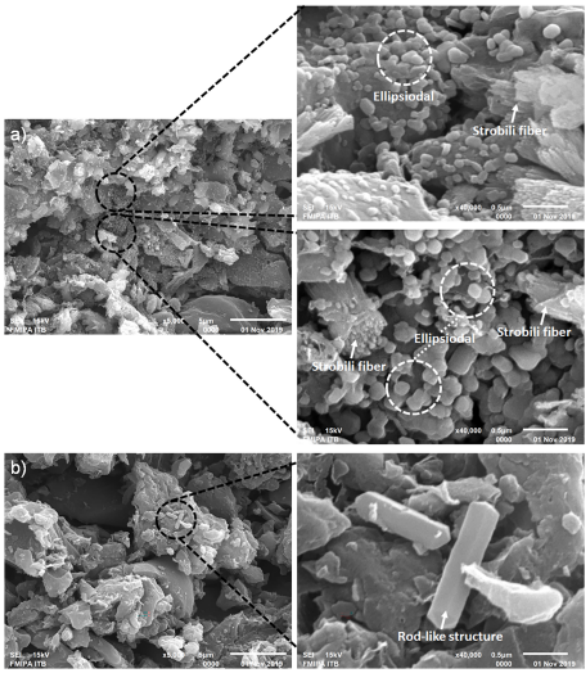

FIG. 4: SEM micrograph images of the MAC-0.5 (a) and MAC-2 (b) samples

MAC-0.5 samples showed an aggregated structure with a size in the range of 0.56–1.29 μm. This structure confirmed the presence of mesopores in the sample. Moreover, the structure had novel ellipsoidal and strobili-fiber morphologies, as shown in the selected area of Fig. 4(a). During the high-temperature pyrolysis process, the volatile content was removed and hemicellulose, cellulose, and lignin were etched from the raw material. The remaining non-volatile fraction of the cocoa shell could be converted into lighter pores that formed on the surface of the biochar. The activation of $ZnCl_2$ possibly extracted the complex compound of biomass including hemicellulose, cellulose, and lignin. As is known, cellulose and lignin can contribute to the formation of strobili-fiber and ellipsoidal structures (Sun et al., 2018; Su et al., 2018). This unique structure may have produced a suitable pore of micro-, meso-, and macropores in the surface of the samples, which provided more active sites for ion diffusion into the electrolyte/electrode interface. This analysis was confirmed by N_2 gas adsorption/desorption. In comparison, the addition of concentrated $ZnCl_2$ in the MAC-2 samples showed a relatively smooth surface structure with a large aggregate size in the range of 0.91–1.79 μm. This may have increased the pore size of the mesopores to macropores in the sample. Its larger size contributed to the provision of pathways for the transport of ions within the electrode material. This analysis was confirmed by its size distribution, which showed the expansion of the average pore diameter of the MAC-2 samples, as seen in Table 2. Furthermore, a rod-like structure was observed on the MAC-2 samples, as seen in the area marked in Fig. 4(b). This was due to the reduction of ellipsoidal and strobili fibers as a result of the addition of the $ZnCl_2$ activator. The ellipsoidal structure was decreased and the strobili fibers were scraped off to form a rod-like structure (Jiang et al., 2019). All of these results were purely derived from changing the cocoa shell waste into activated carbon through $ZnCl_2$ activation without the addition of synthetic materials or metal templates.

3.4 Analysis of the Porous Texture Structure

To further investigate the porous structures of the cocoa shell activated carbon obtained through $ZnCl_2$ activation, the N_2 gas absorption/desorption isotherm was analyzed in detail. As illustrated in Fig. 5(a), the curves of the samples show a combination of type I and IV isotherms, which implies the coexistence of hierarchical pores of micro/mesopores (Fu et al., 2018; Gou et al., 2020). Rapid and obvious adsorption, which was

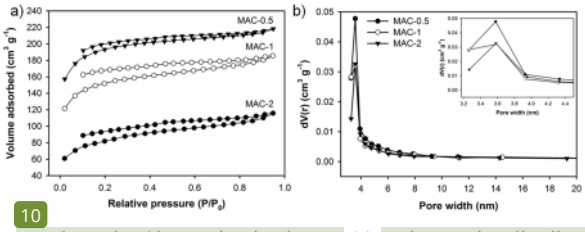

FIG. 5: N_2 adsorption/desorption isotherms (a) and pore size distribution (b)

observed to be at a low relative pressure of 0.1, indicated abundant micropores. On the contrary, the hysteresis loop, which appeared to be in the pressure range of 0.39–0.89, confirmed the mesopores in the samples (Sing, 1982; Yin et al., 2016). Furthermore, the pressure range of 0.89–0.99 demonstrated the existence of macropores (Sing, 1982; Wei et al., 2019). The MAC-0.5 samples showed an enclosed hysteresis loop, which represented the occurrence of the phenomenon of capillary condensation and the formation of numerous mesopores. Furthermore, the MAC-1 and MAC-2 samples showed open hysteresis loops, which were likely caused by the pores being similar to a bottle with a narrow pore neck that allows it to retain N_2 gas until the desorption process is complete (Ayinla et al., 2019). This phenomenon increased the pore size, as confirmed by the average pore diameter (Table 1). The activation of $ZnCl_2$ successfully generated a high specific capacity of activated carbon from the monolithic cocoa shell (up to 619.717 m^2/g^{-1}), as confirmed by the MAC-0.5 samples. This was achieved by combining the unique structure of ellipsoidal and strobili fibers, which provided the highest specific surface area for the MAC-0.5 samples. However, the addition of concentrated $ZnCl_2$ in the MAC-1 and MAC-2 samples reduced the specific surface area, as seen in Table 2. This is because more $ZnCl_2$ can increase the pore size, which may result in several pores collapsing and a decrease in the specific surface area and its distribution, as shown in Fig. 5(b). The pore distribution was centered at approximately 3.2 nm, which was also within the weak and negligible range of 4–19 nm. The activated MAC-0.5 samples exhibited a larger specific surface area and volume adsorption compared to the MAC-1 and MAC-2 samples, which are listed in Table 1. The specific surface area and volume adsorption of the MAC-0.5 samples were calculated as 619.717 m^2/g^{-1} and 0.3385 cm^3/g^{-1}, respectively. However, the MAC-1 and MAC-2 samples showed decreases in the specific surface area and volume adsorption. This confirmed that a low $ZnCl_2$ concentration can easily react in carbon to activate its monolith, and thus improve the specific surface area and volume adsorption (Ahmed et al., 2019; Chiu and Lin, 2019). However, as the value increases, an excess amount of $ZnCl_2$ can corrode the pores' wall and several of them can collapse, which results in enlargement of the pores (He et al., 2013). In addition, to improve the electrochemical performance, the monolith should have a good combination of pore sizes that includes micro-, meso-, and macropores, since micropores can provide more active sites for ions to diffuse into the electrode/electrolyte interface and produce more electrical double layers (Boujibar et al., 2019; He et al.,

TABLE 1: Characteristics of the porous textural structure

Sample	S_{BET} (m^2/g^{-1})	S_{mic} (m^2/g^{-1})	S_{meso} (m^2/g^{-1})	V_{tot} (cm^3/g^{-1})	V_{mic} (cm^3/g^{-1})	V_{meso} (cm^3/g^{-1})	$D_{average}$ (nm)
MAC-0.5	619.717	590.440	29.268	0.3385	0.2947	0.0438	2.185
MAC-1	493.177	460.961	32.216	0.2878	0.2389	0.0489	2.354
MAC-2	247.471	226.426	21.045	0.1796	0.1494	0.0302	2.617

$D_{average}$, average diameter pores; S_{meso}, surface area of mesopores; S_{mic}, surface area of micropores; V_{meso}, mesopores volume; V_{mic}, micropores volume; V_{tot}, total volume.

TABLE 2: The elemental composition of the cocoa shell activated carbon monolith

Elemental Composition	Atomic Weight (%)	
	MAC-0.5	MAC-2
Carbon	92.71	88.79
Oxygen	6.12	9.27
Magnesium	0.24	0.55
Chlorine	0.00	0.21
Potassium	0.16	0.25
Calcium	0.59	0.93

2013). A combination of meso- and macropores has been shown to exhibit good transfer ion pathways for electrolysis, which can boost the current density of a supercapacitor, resulting in high-power density (Zhang et al., 2017; Lin et al., 2019). Furthermore, the highest specific surface area in this study was larger than that used in a previous research study in which cocoa shells were used as the raw material to activate carbon through various methods (Ahmad et al., 2013).

3.5 Analysis of the Composition of the Elements

Elemental analysis was performed to determine the composition of the activated carbon monolith. As shown in Table 2, the elemental composition of the MAC-0.5 samples was dominated by 92.71% of carbon. This high percentage implies that most of the volatile and non-carbon content of the sample had been removed during the activation process, which may provide high conductivity and stability of the cycle for the electrode material (Wei et al., 2019). In addition, the MAC-2 samples had a lower carbon content of up to 88.79%. This was due to the high oxygen content, resulting in the formation of oxide compounds such as CaO and CaCO3, which was confirmed by the degree of crystallinity analysis (Wei et al., 2019). However, the oxygen content favored the wettability, which affected the electrochemical properties. Furthermore, small amounts of other elements (magnesium, chlorine, potassium, and calcium) were found in the MAC samples, since these elements were present in the organic material itself (Contescu et al., 2018). The presence of these elements confirmed the analysis of the degree of crystallinity previously discussed.

3.6 Electrochemical Performance Analysis

To evaluate the electrochemical performance of the activated carbon monolith for the supercapacitor, its electrode was measured using cyclic voltammetry in a two-electrode system with 1 M H_2SO_4 electrolyte. Therefore, the electrodes were tested under a voltage window of 0–1.0 V. The CV profiles of the three MAC samples are shown in Fig. 6(a). The profiles of the MAC-0.5, MAC-1, and MAC-2 samples had

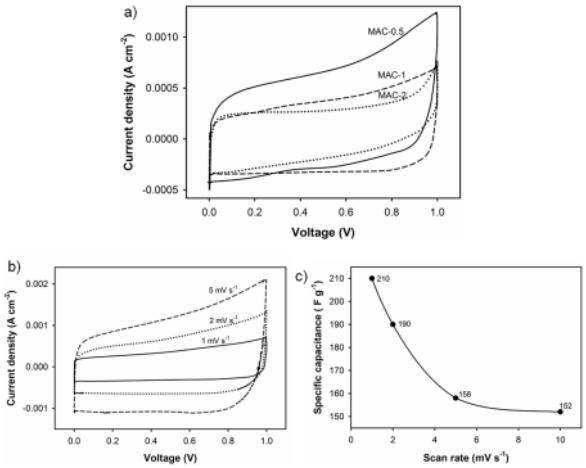

FIG. 6: CV curve of electrodes in the supercapacitor cell (a), CV curve of the MAC-0.5 samples when the scanning rate was increased from 1 to 5 mV/s^{-1} (b), and specific capacitance as a function of the scanning rate for the MAC-0.5 electrode (c)

normal quasi-rectangular shapes, which confirmed good electrochemical double-layer capacitor behavior. However, the CV curves showed an almost non-deformed curvature, which mainly affected the good conductivity of the samples. The CV profile of the MAC-0.5 samples was the largest region, which represented the highest specific capacitance, followed by the MAC-1 and MAC-2 samples. According to Eq. (1), the specific capacitances of the MAC-0.5, MAC-1, and MAC-2 samples were 210, 169, and 93 F/g^{-1}, respectively. The MAC-0.5 samples exhibited the highest specific capacitance compared to the MAC-1 and MAC-2 samples due to their largest specific surface areas and abundant micropores. As previously discussed, the large surface area and abundant micropores and mesopores of the MAC-0.5 samples are beneficial in improving the contact and accumulation of more electrolytes, resulting in high charge storage density. Meanwhile, these mesopores facilitate the rapid diffusion of H_2SO_4 ions in their pore channels, leading to high power density. In addition, the unique structures of the ellipsoidal and strobili fibers contribute to the accessibility of active surface areas (Lebedeva et al., 2015; Zhang et al., 2017). Moreover, the MAC-0.5 samples also exhibited the best amorphous behavior and highest carbon content compared to the MAC-1 and MAC-2 samples, which contributed to boosting the electrochemical behaviors. Table 3 compares the performance of the MAC-0.5 samples with other carbon porous samples based on different raw materials. The CV curves of the performance of the MAC-0.5 samples at different scan rates are shown in Fig. 6(b), where it can be seen that the CV curves maintain approximately quasi-rectangular shapes at 5 mV/s^{-1}. This was mainly due to the pore structure and the abundant micropores, as well as the mesopores, which provided a relatively short distance for

TABLE 3: Comparison between the physical and electrochemical properties of other material sources

Material source	Preparation method	Surface morphological structure	S_{BET} (m^2/g^{-1})	Electrolyte	Electrode system	C_{sp} (F/g^{-1})	Ref.
Cotonier strobili fibers	KOH activation	Strobili fiber	2670.8	6 M KOH	Three electrodes	346.1	Su et al. (2018)
Aluminum hydroxide and trimesic acid	Carbonization and dissolving process	Ellipsoidal structure	1400	6 M KOH	Three electrodes	306.4	Sun et al. (2018)
Al-based metal organic frameworks	Carbonization and KOH-KNO_3 activation	Rod-like structure	1886	6 M KOH	Three electrodes	345	Jiang et al. (2019)
Butnea monsperma flower pollens	$ZnCl_2$ activation	—	1422	6 M KOH	Two electrodes	130	Ahmed et al. (2019)
Durian shell	Single-step carbonization activation	—	—	1 M H_2SO_4	Two electrodes	130.35	Taer et al. (2019)
Cocoa peel	KOH–CO_2 activation	—	—	1 M H_2SO_4	Two electrodes	90.2	Yetri et al. (2020)
Tobacco waste	Hydrothermal treatment and KOH activation	—	111.25	6 M KOH	Three electrodes	148	Chen et al. (2017)
Pineapple leaf	Hydrothermal treatment and KOH activation	Interconnected open-channel nanosheet	1681	1 M H_2SO_4	Three electrodes	202	Sodtipinta et al. (2017)
Hemp (*Cannabis sativa L.*)	KOH activation	Spheres	3062	6 M KOH	Three electrodes	318	Wang et al. (2015)
Sakura flower	KOH activation	Three-dimensional honeycombs	1785.41	6 M KOH	Three electrodes	265.8	Ma et al. (2019a)
Cotton waste	MgO template and $ZnCl_2$ activation	Rod-like structure	1990	6 M KOH	Three electrodes	240	Sun et al. (2019)

TABLE 3: (*continued*)

Material source	Preparation method	Surface morphological structure	S_{BET} (m^2/g^{-1})	Electrolyte	Electrode system	C_{sp} (F/g^{-1})	Ref.
Typha Orientalis	Carbonization and activation	Bamboo-like structure	2797	6 M KOH	Three electrodes	351	Ma et al. (2019b)
Cocoa shell	One-stage integrated pyrolysis and $ZnCl_2$ activation	Ellipsoidal/strobili fiber	619.717	1 M H_2SO_4	Two electrodes	210	This study

—, reported not mention their specific surface area value S_{BET}.
Note: KNO_3, potassium nitrate; KOH, potassium hydroxide; MgO, magnesium oxide.

the ions diffusing at the electrolyte/electrode interface. However, this phenomenon decreased the specific capacitance as the scan rate increased, as shown in Fig. 6(c). The specific capacitance was reduced from 210 F/g^{-1} at 1 mV/s^{-1} to 152 F/g^{-1} at 5 mV/s^{-1}. This may have been caused by the electrolyte ions not having enough time to move into the available pores as well as an increase in the redox reaction in the outer surface of the electrode carbon monolith (Pourhosseini et al., 2017). According to Eqs. (2) and (3), for the MAC-0.5 MAC-1 and MAC-2 samples, the energy densities were 29.16, 23.47, and 12.92 $(W \cdot h)/kg^{-1}$ and the high-power densities were 105.08, 84.57, and 46.54 W/kg^{-1}, respectively. These results were similar to those previously reported, which showed porous activated carbon from bamboo with specific energy and specific power of 10.9 and 63 W/kg^{-1}, respectively (Zhang et al., 2018). For comparison, Table 4 gives a summary of the unique morphological structure [Brunauer–Emmett–Teller surface area (S_{BET})] and the specific capacitance of activated carbon derived from different material sources. However, the specific capacitance of the activated carbon of cocoa is relatively high, even when the specific surface area is smaller than 1000 m^2/g^{-1}. This may be due to several possibilities, such as the unique morphological structure of the ellipsoidal/strobili fiber, which contributed to increased conductivity in the material. In addition, when preparing electrode samples for CV tests, no adhesive material such as polytetrafluoroethylene was used, which is an insulator; therefore, samples without adhesive materials could retain their high conductivity.

4. CONCLUSIONS

Cocoa shell waste–based porous activated carbon was examined and analyzed for its potential use through surface modification as electrodes of supercapacitors. The optimized carbon was discovered in the MAC-0.5 samples, which had an ellipsoidal and strobili-fiber structure and used a combination of large micropores and mesopores. However, the MAC-2 sample exhibited a rod-like structure. All of these unique structures helped to improve the specific surface area and the appropriate pore size distribution, which enhanced the electrochemical performance of the supercapacitor electrodes. Furthermore, the symmetrical supercapacitor in monolithic forms achieved high electrochemical behavior with higher specific capacitances of 210 F/g^{-1} in the two-electrode system. Due to the unique and high electrochemical properties of activated carbon with simple processing, cocoa waste becomes a potential material for use in supercapacitor electrodes.

ACKNOWLEDGMENT

This research was financially supported by a first year Project of Penelitian Dasar Unggulan Perguruan Tinggi (PDUPT) in Kementerian Pendidikan Kebudayaan Riset dan Teknologi, Republic of Indonesia (Contract No. 457/UN.19.5.1.3/PT.01.03/2021), with the title "Synthesis of Nano Carbon Biomass Waste-based as Raw Material of Supercapacitor Electrodes with High Energy and Power Densities."

REFERENCES

Abbas, Q., Raza, R., Shabbir, I., and Olabi, A.G., Heteroatom Doped High Porosity Carbon Nanomaterials as Electrodes for Energy Storage in Electrochemical Capacitors: A Review, *J. Sci.: Adv. Mater. Devices*, vol. **4**, no. 3, pp. 341–352, 2019.

Ahmad, F., Daud, W.M.A.W., Ahmad, M.A., Radzi, R., and Azmi, A.A., The Effects of CO_2 Activation, on Poro and Surface Functional Groups of Cocoa (Theobroma Cacao) – Shell Based Activated Carbon, *J. Environ. Chem. Eng.*, vol. **1**, no. 3, pp. 378–388, 2013.

Ahmed, S., Ahmed, A., and Rafat, M., Investigation on Activated Carbon Derived from Biomass Butnea Monosperma and Its Application as a High Performance Supercapacitor Electrode, *J. Energy Storage*, vol. **26**, p. 100988, 2019.

Avcıoğlu, A.O., Dayıoğlu, M.A., and Türker, U., Assessment of the Energy Potential of Agricultural Biomass Residues in Turkey, *Renew. Energy*, vol. **138**, pp. 610–619, 2019.

Ayinla, R.T., Dennis, J.O., Zaid, H.M., Sanusi, Y.K., Usman, F., and Adebayo, L.L., A Review of Technical Advances of Recent Palm Bio-Waste Conversion to Activated Carbon for Energy Storage, *J. Cleaner Prod.*, vol. **229**, pp. 1427–1442, 2019.

Bilandzija, N., Voca, N., Jelcic, B., Jurisic, V., Matin, A., Grubor, M., and Kricka, T., Evaluation of Croatian Agricultural Solid Biomass Energy Potential, *Renew. Sust. Energ. Rev.*, vol. **93**, pp. 225–230, 2018.

Boujibar, O., Ghosh, A., Achak, O., Chafik, T., and Ghamouss, F., A High Energy Storage Supercapacitor Based on Nanoporous Activated Carbon Electrode Made from Argan Shells with Excellent Ion Transport in Aqueous and Non-Aqueous Electrolytes, *J. Energy Storage*, vol. **26**, p. 100958, 2019.

Boyjoo, Y., Chen , Zhong, H., Tian, H., Pan, J., Pareek, V.K., Jiang, S.P., Lamonier, J.-F., Jaroniec, M., and Liu, J., From Waste Coca Cola® to Activated Carbons with Impressive Capabilities for CO_2 Adsorption and Supercapacitors, *Carbon*, vol. **116**, pp. 490–499, 2017.

Chen, H., Guo, Y.C., Wang, F., Wang, G., Qi, P.R., Guo, X.H., Dai, B., and Yu, F., An Activated Carbon Derived from Tobacco Waste for Use as a Supercapacitor Electrode Material, *New Carbon Mater.*, vol. **32**, no. 6, pp. 592–599, 2017.

Chiu, Y.-H. and Lin, L.-Y., Effect of Activating Agents for Producing Activated Carbon Using a Facile One-Step Synthesis with Waste Coffee Grounds for Symmetric Supercapacitors, *J. Taiwan Inst. Chem. Eng.*, vol. **101**, pp. 177–185, 2019.

Contescu, C.I., Adhikari, S.P., Gallego, N.C., and Evans, N.D., Activated Carbons Derived from High-Temperature Pyrolysis of Lignocellulosic Biomass, *J. Carbon Res.*, vol. **4**, no. 511, pp. 9–13.

Dehkhoda, A.M., Gyenge, E., and Ellis, N., A Novel Method to Tailor the Porous Structure of KOH-Activated Biochar and Its Application in Capacitive Deionization and Energy Storage, *Biomass Bioenergy*, vol. **87**, pp. 107–121, 2016.

Dessie, Y., Tadesse, S., Eswaramoorthy, R., and Abebe, B., Recent Developments in Manganese Oxide Based Nanomaterials with Oxygen Reduction Reaction Functionalities for Energy Conversion and Storage plications: A Review, *J. Sci.: Adv. Mater. Devices*, vol. **4**, no. 3, pp. 353–369, 2019.

Fan, Y., Cai, Y., Li, X., Jiao, L., Xia, J., and Deng, X., Effects of the Cellulose, Xylan and Lignin Constituents on Biomass Pyrolysis Characteristics and Bio-Oil Composition Using the Simplex Lattice Mixture Design Method, *Energy Convers. Manage.*, vol. **138**, pp. 106–118, 2017.

Fioresi, F., Vieillard, Bargougui, R., Bouazizi, N., Fotsing, P.N., Woumfo, E.D., Brun, N., Mofaddel, N., and Le Derf, F., Chemical Modification of the Cocoa Shell Surface Using Diazonium Salts, *J. Colloid Interface Sci* ol. **494**, pp. 92–97, 2017.

Fu, Y., Zhang, N., Shen, Y., Ge, X., and Chen, M., Micro-Mesoporous Carbons from Original and Pelletized Rice Husk via One-Step Catalytic Pyrolysis, *Bioresour. Technol.*, vol. **269**, pp. 67–73, 2018.

Gao, Z., Zhang, Y., Song, N., and Li, X., Biomass-Derived Renewable Carbon Materials for Electrochemical Energy Storage, *Mater. Res. Lett.*, vol. **5**, no. 2, pp. 69–88, 2017.

González, A., Goikolea, E., Barrena, J.A., and Mysyk, R., Review on Supercapacitors: Technologies and Materials, *Renew. Sust. Energ. Rev.*, vol. **58**, pp. 1189–1205, 2016.

González, J.F., Román, S., Encinar, J.M., and Martínez, G., Pyrolysis of Various Biomass Residues and Char Utilization for the Production of Activated Carbons, *J. Anal. Appl. Pyrolysis*, vol. **85**, no. 1–2, pp. 134–141, 2009.

González-García, P., Activated Carbon from Lignocellulosics Precursors: A Review of the Synthesis Methods, Characterization Techniques and Applications, *Renew. Sust. Energ. Rev.*, vol. **82**, pp. 1393–1414, 2018.

Gou, G., Huang, F., Jiang, M., Li, J., and Zhou, Z., Hierarchical Porous Carbon Electrode Materials for Supercapacitor Developed from Wheat Straw Cellulosic Foam, *Renew. Energ.*, vol. **149**, pp. 208–216, 2020.

He, X., Li, R., Han, J., Yu, M., and Wu, M., Facile Preparation of Mesoporous Carbons for Supercapacitors by One-Step Microwave-Assisted $ZnCl_2$ Activation, *Mater. Lett.*, vol. **94**, pp. 158–160, 2013.

Jain, A., Xu, C., Jayaraman, S., Balasubramanian, R., Lee, J.Y., and Srinivasan, M.P., Mesoporous Activated Carbons with Enhanced Porosity by Optimal Hydrothermal Pre-Treatment of Biomass for Supercapacitor Applications, *Microporous Mesoporous Mater.*, vol. **218**, pp. 55–61, 2015.

Jawad, A.H., Bardhan, , Islam, M.A., Islam, M.A., Syed-Hassan, S.S.A., Surip, S.N., ALOthman, Z.A., and Khan, M.R., Insights into the Modeling, Characterization and Adsorption Performance of Mesoporous Activated Carbon from Corn Cob Residue via Microwave-Assisted H_3PO_4 Activation, *Surf. Interfaces*, vol. **21**, p. 100688, 2020.

Jiang, W., Pan, J., and Liu, X., A Novel Rod-Like Porous Carbon with Ordered Hierarchical Pore Structure Prepared from Al-Based Metal-Organic Framework without Template as Greatly Enhanced Performance for Supercapacitor, *J. Power Sources*, vol. **409**, pp. 13–23, 2019.

Jose, J., Thomas, V., Vinod, V., Abraham, R., and Abraham, S., Nanocellulose Based Functional Materials for Supercapacitor Applications, *J. Sci.: Adv. Mater. Devices*, vol. **4**, no. 3, pp. 333–340, 2019.

Kirbiyik, Ç., Pütün, A.E., and Pütün, E., Equilibrium, Kinetic, and Thermodynamic Studies of the Adsorption of Fe(III) Metal Ions and 2,4-Dichlorophenoxyacetic Acid onto Biomass-Based Activated Carbon by $ZnCl_2$ Activation, *Surf. rfaces*, vol. **8**, no. 3, pp. 182–192, 2017.

Kumar, A. and Samadder, S.R., A Review on Technological Options of Waste to Energy for Effective Management of Municipal Solid Waste, *Waste Manage.*, vol. **69**, pp. 407–422, 2017.

Lebedeva, M.V., Yeletsky, P.M., Ayupov, A.B., Kuznetsov, A.N., Yakovlev, V.A., and Parmon, V.N., Micro–Mesoporous Carbons from Rice Husk as Active Materials for Supercapacitors, *Mater. Renew. Sustain. Energy*, vol. **4**, no. 4, pp. 1–9, 2015.

Li, Y., Wang, X., and Cao, M., Three-Dimensional Porous Carbon Frameworks Derived from Mangosteen Peel Waste as Promising Materials for CO_2 Capture and Supercapacitors, *J. CO2 Util.*, vol. **27**, pp. 204–216, 2018.

Lin, X.-Q., Yang, N., Lü, Q.-F., and Liu, R., Self-Nitrogen-Doped Porous Biocarbon from Watermelon Rind: A High-Performance Supercapacitor Electrode and Its Improved Electrochemical Performance Using Redox Additive Electrolyte, *Energy Technol.*, vol. **7**, no. 3, p. 1800628, 2019. DOI: 10.1002/ente.201800628

Liu, X., Zhang, S., and Bae, J., The Nexus of Renewable Energy-Agriculture-Environment in BRICS, *Appl. Energy*, vol. **204**, pp. 489–496, 2017.

Liu, Y., Chen, J., Cui, B., Yin, P., and Zhang, C., Design and Preparation of Biomass-Derived Carbon Materials for Supercapacitors: A Review, *J. Carbon Res.*, vol. **4**, no. 4, p. 53, 2018.

Lu, W., Cao, X., Hao, L., Zhou, Y., and Wang, Y., Activated Carbon Derived from Pitaya Peel for Supercapacitor Applications with High Capacitance Performance, *Mater. Lett.*, vol. **264**, p. 127339, 2020.

Ma, F., Ding, S., Ren, H., and Liu, Y., Sakura-Based Activated Carbon Preparation and Its Performance in Supercapacitor Applications, *RSC Adv.*, vol. **9**, no. 5, pp. 2474–2483, 2019a.

Ma, X., Wang, H., Wu, Q., Zhang, J., Liang, D., Lu, S., and Xiang, Y., Bamboolike Carbon Microfibers Derived from *Typha Orientalis* Fibers for Supercapacitors and Capacitive Deionization, *J. Electrochem. Soc.*, vol. **166**, no. 2, pp. A236–A244, 2019b.

Mai, T.-T., Vu, D.-L., Huynh, D.-C., Wu, N.-L., and Le, A.-T., Cost-Effective Porous Carbon Materials Synthesized by Carbonizing Rice Husk and K_2CO_3 Activation and Their Application for Lithium-Sulfur Batteries, *J. Sci.: Adv. Mater. Devices*, vol. **4**, no. 2, pp. 223–2[illegible] 2019.

Men, B., Guo, P., Sun, Y., Tang, Y., Chen, Y., Pan, J., and Wan, P., High-Performance Nitrogen-Doped Hierarchical Porous Carbon Derived from Cauliflower for Advanced Supercapacitors, *J. Mater. Sci.*, vol. **54**, no. 3, pp. 2446–2457, 2019.

Miller, E.E., Hua, Y., and Tezel, F.H., Materials for Energy Storage: Review of Electrode Materials and Methods of Increasing Capacitance for Supercapacitors, *J. Energy Storage*, vol. **20**, pp. 30–40, 2018.

Okiyama, D.C.G., Navarro, S.L.B., and Rodrigues, C.E.C., Cocoa Shell and Its Compounds: Applications in the Food Industry, *Trends Food Sci. Technol.*, vol. **63**, pp. 103–112, 2017.

Pereira, R.G., Veloso, C.M., da Silva, N.M., de Sousa, L.F., [illegible]nomo, R.C.F., de Souza, A.O., da Guarda Souza, M.O., and da Costa Ilhéu Fontan[illegible]., Preparation of Activated Carbons from Cocoa Shells and Siriguela Seeds Using H_3PO_4 and $ZnCl_2$ as Activating Agents for BSA and α-Lactalbumin Adsorption, *Fuel Process. Technol.*, vol. **126**, pp. 476–486, 2014.

Poonam, Sharma, K., Arora, A., and Tripathi, S.K., Review of Supercapacitors: Materials and Devices, *J. Energy Storage*, vol. **21**, pp. 801–825, 2019.

Pourhosseini, S.E.M., Norouzi, O., and Naderi, H.R., Study of Micro/Macro Ordered Porous Carbon with Olive-Shaped Structure Derived from *Cladophora Glomerata* Macroalgae as Efficient Working Electrodes of Supercapacitors, *Biomass Bioenergy*, vol. **107**, [illegible]287–298, 2017.

Qu, W.-H., Xu, Y.-Y., Lu, A.-N., Zhang, X.-Q., and Li, W., Converting Biowaste Corncob Residue into High Value Added Porous Carbon for Supercapacitor Electrodes, *Bioresour. Technol.*, vol. **189**, pp. 285–291, 2015.

Rountree, V., Nevada's Experience with the Renewable Portfolio Standard, *Energy Policy*, vol. **129**, pp. 279–[illegible], 2019.

Saka, C., BET, TG–DTG, FT-IR, SEM, Iodine Number Analysis and Preparation of Activated Carbon from Acorn Shell by Chemical Activation with $ZnCl_2$, *J. Anal. Appl. Pyrolysis*, vol. **95**, pp. 21–24, 2012.

Simon, P. and Burke, A., Nanostructured Carbons: Double-Layer Capacitance and More, *Electrochem. Soc. Interface*, vol. **17**, no. 1, pp. 38–43, 2008.

Sing, K.S.W., Reporting Physisorption Data for Gas/Solid Systems with Special Reference to the Determination of Surface Area and Porosity, *Pure Appl. Chem.*, vol. **54**, no. 11, pp. 2201–2218, 1982.

Sodtipinta, J., Ieosakulrat, C., Poonyayant, N., Kidkhunthod, P., Chanlek, N., Amornsakchai, T., and Pakawatpanurut, P., Interconnected Open-Channel Carbon Nanosheets Derived from Pineapple Leaf Fiber as a Sustainable Active Material for Supercapacitors, *Ind. Crops Prod.*, vol. **104**, pp. 13–20, 2017.

Su, X.-L., Li, S.-H., Jiang, S., Peng, Z.-K., Guan, X.-X., and Zheng, X.-C., Superior Capacitive Behavior of Porous Activated Carbon Tubes Derived from Biomass Waste-Cotonier Strobili Fibers, *Adv. Powder Technol.*, vol. **29**, no. 9, pp. 2097–[illegible]7, 2018.

Sun, Q., Jiang, T., Zhao, G., and Shi, J., Porous Carbon Material Based on Biomass Prepared by MgO Template Method and $ZnCl_2$ Activation Method as Electrode for High Performance Supercapacitor, *Int. J. Electrochem. Sci.*, vol. **14**, no. 1, pp. 1–14, 2019.

Sun, Y., Guo, S., Li, W., Pan, J., Fernandez, C., Senthil, R.A., and Sun, X., A Green and Template-Free Synthesis Process of Superior Carbon Material with Ellipsoidal Structure as Enhanced Material for Supercapacitors, *J. Power Sources*, vol. **405**, pp. 80–88, 2018.

Taer, E, Apriwandi, A., Dalimunthe, B.K.L., and Taslim, R., A Rod-Like Mesoporous Carbon Derived from Agro-Industrial Cassava Petiole Waste for Supercapacitor Application, *J. Chem. Technol. Biotechnol.*, vol. **96**, no. 3, pp. 662–671, 2021.

Taer, E, Apriwandi, A., Taslim, R., Malik, U., and Usman, Z., Single Step Carbonization-Activation of Durian Shells for Producing Activated Carbon Monolith Electrodes, *Int. J. Electrochem. Sci.*, vol. **14**, pp. 1318–1330, 2019.

Thomas, P., Lai, C.W., and Bin Johan, M.R., Recent Developments in Biomass-Derived Carbon as a Potential Sustainable Material for Super-Capacitor-Based Energy Storage and Environmental Applications, *J. Anal. Appl. Pyrolysis*, vol. **140**, pp. 54–85, 2019.

Uysal, T., Duman, G., Onal, Y., Yasa, I., and Yanik, J., Production of Activated Carbon and Fungicidal Oil from Peach Stone by Two-Stage Process, *J. Anal. Appl. Pyrolysis*, vol. **108**, pp. 47–55, 2014.

Vásquez, Z.S., de Carvalho Neto, D.P., Pereira, G.V.M., Vandenberghe, L.P.S., de Oliveira, P.Z., Tiburcio, P.B., Rogez, H.L.G., Góes Neto, A., and Soccol, C.R., Biotechnological Approaches for Cocoa Waste Management: A Review, *Waste Manage.*, vol. **90**, pp. 72–83, 2019.

Wang, B., Dong, F., Chen, M., Zhu, J., Tan, J., Fu, X., Wang, Y., and Chen, S., Advances in Recycling and Utilization of Agricultural Wastes in China: Based on Environmental Risk, Crucial Pathways, Influencing Factors, Policy Mechanism, *Procedia Environ. Sci.*, vol. **31**, pp. 12–17, 2016.

Wang, Y., Qu, Q., Gao, S., Tang, G., Liu, K., He, S., and Huang, C., Biomass Derived Carbon as Binder-Free Electrode Materials for Supercapacitors, *Carbon*, vol. **155**, pp. 706–726, 2019.

Wang, Y., Yang, R., Li, M., and Zhao, Z., Hydrothermal Preparation of Highly Porous Carbon Spheres from Hemp (Cannabis Sativa L.) Stem Hemicellulose for Use in Energy-Related Applications, *Ind. Crops Prod.*, vol. **65**, pp. 216–226, 2015.

Wei, X., Wei, J.-S., Li, Y., and Zou, H., Robust Hierarchically Interconnected Porous Carbons Derived from Discarded Rhus Typhina Fruits for Ultrahigh Capacitive Performance Supercapacitors, *J. Power Sources*, vol. **414**, pp. 13–23, 2019.

Yang, V., Senthil, R.A., Pan, J., Khan, A., Osman, S., Wang, L., Jiang, W., and Sun, Y., Highly Ordered Hierarchical Porous Carbon Derived from Biomass Waste Mangosteen Peel as Superior Cathode Material for High Performance Supercapacitor, *J. Electroanal. Chem.*, vol. **855**, p. 113616, 2019.

Yetri, Y., Mursida, Dahlan, D., Taer, E., Agustino, and Muldarisnur, Identification of Cacao Peels Potential as a Basic of Electrodes Environmental Friendly Supercapacitors, *Key Eng. Mater.*, vol. **846**, pp. 274–281, 2020.

Yin, L., Chen, Y., Li, D., Zhao, X., Hou, B., and Cao, B., 3-Dimensional Hierarchical Porous Activated Carbon Derived from Coconut Fibers with High-Rate Performance for Symmetric Supercapacitors, *Mater. Des.*, vol. **111**, pp. 44–50, 2016.

Zhang, G., Chen, Y., Chen, Y., and Guo, H., Activated Biomass Carbon Made from Bamboo as Electrode Material for Supercapacitors, *Mater. Res. Bull.*, vol. **102**, no. 2010, pp. 391–398, 2018.

Zhang, Y., Yu, S., Lou, G., Shen, Y., Chen, H., Shen, Z., Zhao, S., Zhang, J., Chai, S., and Zou, Q., Review of Macroporous Materials as Electrochemical Supercapacitor Electrodes, *J. Mater. Sci.*, vol. **52**, no. 19, pp. 11201–11228, 2017.

SURFACE MODIFICATION: UNIQUE ELLIPSOIDAL/STROBILI-FIBER STRUCTURE OF POROUS CARBON MONOLITH FOR ELECTRODE SUPERCAPACITOR

ORIGINALITY REPORT

11%	7%	5%	4%
SIMILARITY INDEX	INTERNET SOURCES	PUBLICATIONS	STUDENT PAPERS

PRIMARY SOURCES

1	aperta.ulakbim.gov.tr Internet Source	<1%
2	insightsociety.org Internet Source	<1%
3	knepublishing.com Internet Source	<1%
4	nrl.northumbria.ac.uk Internet Source	<1%
5	scholarworks.unist.ac.kr Internet Source	<1%
6	www.agrojournal.org Internet Source	<1%
7	www.eeer.org Internet Source	<1%
8	Submitted to University of Teesside Student Paper	<1%

9	Xianjin Cui, Markus Antonietti, Shu-Hong Yu. "Structural Effects of Iron Oxide Nanoparticles and Iron Ions on the Hydrothermal Carbonization of Starch and Rice Carbohydrates", Small, 2006 Publication	<1 %
10	Xiaojun He, Ruchun Li, Jiufeng Han, Moxin Yu, Mingbo Wu. "Facile preparation of mesoporous carbons for supercapacitors by one-step microwave-assisted ZnCl2 activation", Materials Letters, 2013 Publication	<1 %
11	blog.ump.edu.my Internet Source	<1 %
12	riafsg.uitm.edu.my Internet Source	<1 %
13	trepo.tuni.fi Internet Source	<1 %
14	www.agr.unizg.hr Internet Source	<1 %
15	www.eng.uwo.ca Internet Source	<1 %
16	Patrice Simon, Thierry Brousse, Frédéric Favier. "Bibliography", Wiley, 2017 Publication	<1 %

17	Wen Wang, Kritsadaporn Porninta, Pruk Aggarangsi, Noppol Leksawasdi et al. "Bioenergy development in Thailand based on the potential estimation from crop residues and livestock manures", Biomass and Bioenergy, 2021 Publication	<1 %
18	bof.fire.ca.gov Internet Source	<1 %
19	www.sciencegate.app Internet Source	<1 %
20	Submitted to TecnoCampus Student Paper	<1 %
21	Submitted to Universiteit Twente Student Paper	<1 %
22	Submitted to University of Technology, Sydney Student Paper	<1 %
23	aunilo.uum.edu.my Internet Source	<1 %
24	hal.univ-lille.fr Internet Source	<1 %
25	mai.group.whut.edu.cn Internet Source	<1 %
26	Submitted to Chungnam National University Student Paper	

		<1%
27	Onal, E.P.. "Steam pyrolysis of an industrial waste for bio-oil production", Fuel Processing Technology, 201105 Publication	<1%
28	etheses.whiterose.ac.uk Internet Source	<1%
29	www.astrj.com Internet Source	<1%
30	Submitted to CSU Northridge Student Paper	<1%
31	Submitted to Gautam Buddha University Student Paper	<1%
32	Submitted to London School of Economics and Political Science Student Paper	<1%
33	Shian Dong, Xiuyan Ji, Moxin Yu, Yuanyang Xie, Dawei Zhang, Xiaojun He. "Direct synthesis of interconnected porous carbon nanosheet/nickel foam composite for high-performance supercapacitors by microwave-assisted heating", Journal of Porous Materials, 2017 Publication	<1%

34	Taer, E.. "Growth of platinum nanoparticles on stainless steel 316L current collectors to improve carbon-based supercapacitor performance", Electrochimica Acta, 20111130 Publication	<1 %
35	Submitted to Universidad Nacional de Colombia Student Paper	<1 %
36	mafiadoc.com Internet Source	<1 %
37	N. Yoshizawa, Y. Yamada, T. Furuta, M. Shiraishi, S. Kojima, H. Tamai, H. Yasuda. "Coal-Based Activated Carbons Prepared with Organometallics and Their Mesoporous Structure", Energy & Fuels, 1997 Publication	<1 %
38	www.mater-rep.com Internet Source	<1 %
39	Submitted to University of Nevada, Las Vegas Student Paper	<1 %
40	Wu, F.C.. "The capacitive characteristics of activated carbons-comparisons of the activation methods on the pore structure and effects of the pore structure and electrolyte on the capacitive performance", Journal of Power Sources, 20060922 Publication	<1 %

41 Xi Li, Jian Li, Lin-Lin Zhu, Ranran He, Zongqun Li, Chuanhu Wang, Boliang Wang. "MOLECULAR DYNAMICS SIMULATIONS OF THE MISCIBILITY AND GLASS TRANSITION TEMPERATURE OF POLYMETHYL METHACRYLATE/ACETYL TRIBUTYL CITRATE BINARY SYSTEMS", International Journal of Energetic Materials and Chemical Propulsion, 2021 <1%
Publication

42 R.A. Mendybaev. "Volatilization kinetics of silicon carbide in reducing gases: an experimental study with applications to the survival of presolar grains in the solar nebula", Geochimica et Cosmochimica Acta, 20020215 <1%
Publication

43 F. Béguin, K. Szostak, G. Lota, E. Frackowiak. "A Self-Supporting Electrode for Supercapacitors Prepared by One-Step Pyrolysis of Carbon Nanotube/Polyacrylonitrile Blends", Advanced Materials, 2005 <1%
Publication

44 Gryglewicz, G.. "Effect of pore size distribution of coal-based activated carbons on double layer capacitance", Electrochimica Acta, 20050115 <1%
Publication

45	Lebedeva, Marina V., Petr M. Yeletsky, Artem B. Ayupov, Aleksey N. Kuznetsov, Vadim A. Yakovlev, and Valentin N. Parmon. "Micro–mesoporous carbons from rice husk as active materials for supercapacitors", Materials for Renewable and Sustainable Energy, 2015. Publication	<1 %
46	Mônica Beatriz Thürmer, Carlos Eduardo Diehl, Fábio José Bento Brum, Luís Alberto dos Santos. "Preparation and characterization of hydrogels with potential for use as biomaterials", Materials Research, 2014 Publication	<1 %
47	Raditya Hendra Pratama, Akira Sou, Tokihiro Katsui, Shigeru Nishio. "STRING CAVITATION IN A FUEL INJECTOR", Atomization and Sprays, 2017 Publication	<1 %
48	Diyan Unmu Dzujah, Abdul-Muizz Pradipto, Rahmat Hidayat, Kohji Nakamura. "Modification of plasmonic properties in several transition metal-doped graphene studied by the first principles method", RSC Advances, 2023 Publication	<1 %
49	Li, Jiangfeng, and Qingsheng Wu. "Water bamboo-derived porous carbons as electrode	<1 %

materials for supercapacitors", New Journal of Chemistry, 2015.
Publication

50	Patricia González, Claudio Zaror, Virginia Carrasco, Maria Angelica Mondaca, Hector Mansilla. "Combined Physical-Chemical and Biological Treatment of Poorly Biodegradable Industrial Effluents", Journal of Environmental Science and Health, Part A, 2003 Publication	<1 %
51	Syunichi Oshima, Jilska M. Perera, Kathy A. Northcott, Hisao Kokusen, Geoffrey W. Stevens, Yu Komatsu. "Adsorption Behavior of Cadmium(II) and Lead(II) on Mesoporous Silicate MCM‐41", Separation Science and Technology, 2006 Publication	<1 %
52	crcu.jlu.edu.cn Internet Source	<1 %
53	www.kiche.or.kr Internet Source	<1 %
54	www.umt.edu Internet Source	<1 %
55	Y Yetri, Mursida, D Dahlan, Muldarisnur, E Taer, Febrielviyenti. "Analysis of Characteristics of Activated Carbon from Cacao (Theobroma cacao) Skin Waste for	<1 %

Supercapasitor Electrodes", IOP Conference Series: Materials Science and Engineering, 2020
Publication

56	digital.library.unt.edu Internet Source	<1%
57	Submitted to Indian Institute of Technology, Kharagpure Student Paper	<1%
58	Portet, C.. "High power density electrodes for Carbon supercapacitor applications", Electrochimica Acta, 20050725 Publication	<1%
59	island.lk Internet Source	<1%
60	moam.info Internet Source	<1%
61	onlineinnovationsjournal.com Internet Source	<1%
62	Taberna, P.L.. "Activated carbon-carbon nanotube composite porous film for supercapacitor applications", Materials Research Bulletin, 20060309 Publication	<1%
63	Robert F Nelson. "Power requirements for batteries in hybrid electric vehicles", Journal of	<1%

Power Sources, 2000

Publication

Exclude quotes	Off	Exclude matches	Off
Exclude bibliography	Off		